REGULAR ARTICLE

blood neoplasia

Epigenetic activation of EBV BGLF4 determines antiviral-based regimen response in EBV+CNS lymphoproliferative disease

Christoph Weigel,[1,*] Haley L. Klimaszewski,[2,*] Fode Tounkara,[3] Selamawit Addissie,[4] Sarah Schlotter,[2] Betsy Pray,[1] James P. Dugan,[5] Bradley M. Haverkos,[6] Lynda Villagomez,[7] Mark Lustberg,[8] Pierluigi Porcu,[9] Timothy Voorhees,[10] Richard F. Ambinder,[11] Shannon C. Kenney,[12] Joyce Fingeroth,[13] Henri-Jacques Delecluse,[14] Michael A. Caligiuri,[15] Lapo Alinari,[1,16] Ginny Bumgardner,[17] Christopher C. Oakes,[1,17,18] and Robert A. Baiocchi[1,16]

[1]Division of Hematology, Department of Internal Medicine, [2]College of Medicine, and [3]Center for Biostatistics, The Ohio State University, Columbus, OH; [4]Department of Internal Medicine, Johns Hopkins University, Baltimore, MD; [5]Malignant Hematology and Cellular Therapy Department, Novant Health Cancer Institute - Forsyth Medical Center, Winston-Salem, NC; [6]Division of Hematology, University of Colorado School of Medicine, Aurora, CO; [7]Division of Hematology and Oncology, Department of Pediatrics, The Ohio State University and Nationwide Children's Hospital, Columbus, OH; [8]Division of Infectious Disease, Department of Internal Medicine, Yale School of Medicine, New Haven, CT; [9]Division of Hematologic Malignancies and Hematopoietic Stem Cell Transplantation, Department of Medical Oncology, Sidney Kimmel Cancer Center, Thomas Jefferson University, Philadelphia, PA; [10]Department of Hematology, James Comprehensive Cancer Center, The Ohio State University, Columbus, OH; [11]Department of Oncology, Johns Hopkins University School of Medicine, Baltimore, MD; [12]Department of Oncology, McArdle Laboratory for Cancer Research, School of Medicine and Public Health, University of Wisconsin Madison, Madison, WI; [13]Department of Medicine, Chan Medical School, University of Massachusetts, Worcester, MA; [14]Pathogenesis of Virus Associated Tumors, German Cancer Research Center, Heidelberg, Germany; [15]Department of Hematology & Hematopoietic Cell Transplantation, City of Hope National Medical Center, Los Angeles, CA; [16]Comprehensive Cancer Center, The James Cancer Hospital and Solove Research Institute, The Ohio State University, Columbus, OH; [17]Comprehensive Transplant Center, Department of Surgery, The Ohio State University College of Medicine, Columbus, OH; and [18]Department of Biomedical Informatics, The Ohio State University, Columbus, OH

Key Points

- Methylation loss and increased expression of EBV *BGLF4* was associated with favorable response to the GARD regimen in aggressive EBV-CNSL.
- Epigenetic regulation of lytic *BGLF4* expression in a latent EBV malignancy supports EBV DNA methylation as a clinically relevant biomarker.

Epstein-Barr virus (EBV)–associated primary central nervous system lymphoproliferative diseases (EBV+PCNSL) are aggressive conditions with poor prognoses. We previously reported durable responses in patients with PCNSL who were treated with the antivirals ganciclovir and azidothymidine, plus rituximab and dexamethasone (GARD). Responses were associated with the detection of the lytic viral protein kinases, BGLF4 and BXLF1. These antiviral activating kinases are associated with lytic EBV, however, the mechanism for expression in latently infected EBV+CNSL is unknown. Expanding on previous work, we provide long-term clinical outcome data (N = 24) and show that RNA expression analysis in CNSL tissue biopsies (n = 12) confirmed the expression of *LMP1*, *BXLF1*, and *BGLF4* but not *BZLF1*, supporting an incomplete lytic EBV program. Control biopsies from systemic PTLD cases (N = 24) showed significantly less expression of *BXLF1* and *BGLF4*. By quantifying DNA methylation in EBV gene promoters, we showed significantly decreased promoter methylation at *BGLF4* in CNSL vs systemic PTLD cases (P = .0006). Luciferase reporter analysis of the *BGLF4* upstream sequence revealed 3 regions of promoter activity, and 5' rapid amplification of complimentary DNA ends in EBV-infected cell lines and CNSL samples identified transcription start sites at these promoters. We identified CNSL-specific DNA methylation loss at single CpG dinucleotides, whereas the surrounding EBV methylation levels remained high. Lastly, *TET* knockout and the expression of TET1/2-suppressive mutant IDH1 in a latent HEK293 EBV model indicated that active

Submitted 27 June 2025; accepted 25 December 2025; prepublished online 28 February 2026. https://doi.org/10.1016/j.bneo.2026.100200.

*C.W. and H.L.K. contributed equally to this study.

Select data that were generated in this study are available within the article and its supplemental files. Additional deidentified data are available on request from the corresponding author, Robert A. Baiocchi (robert.baiocchi@osumc.edu), in compliance with institutional review board approval pertaining to protection of protected patient health information.

The full-text version of this article contains a data supplement.

demethylation is necessary for the activity of *BGLF4* promoters. We detailed the epigenetic basis of *BGLF4* expression in CNSL via locus-specific promoter activation, which may hold value for determining GARD sensitivity.

Introduction

Epstein-Barr virus (EBV) is a gamma herpesvirus that drives a variety of human diseases, including hematologic malignancies.[1] EBV maintains lifelong infection by entering a latency state inside host cells and silencing many of its genetic elements. EBV can undergo lytic activation, which leads to the expression of lytic genes, viral DNA replication, and the release of infectious viral particles.[2] Host epigenetic mechanisms are indispensable for the EBV life cycle.[2,3] Among these, DNA methylation primarily serves as a gene silencing mechanism during EBV latency to suppress lytic transcripts.[4] Lytic activation necessitates the removal of DNA methylation.[2]

The clinical EBV assays currently available only detect the presence of EBV by quantitative polymerase chain reaction (qPCR)[5,6] and do not provide information on EBV gene expression or lytic/latent states. Thus, clinical decision-making based on EBV detection alone has remained challenging. This is particularly true in immunosuppressive states that predispose patients to oncogenesis via latent EBV and lytic viral activation, which often complicates differential diagnosis. Primary central nervous system lymphoproliferative disease (PCNSL) is a group of rare, extranodal lymphomas that are typically linked to preexisting immunosuppression. Of all PCNSL cases, 15% are EBV-associated (EBV+) and exhibit unique genomic and transcriptional landscapes when compared with EBV-negative disease.[7,8] CNS involvement also occurs in 5% to 30% of posttransplant lymphoproliferative disease (PTLD) and is overwhelmingly EBV+.[7] EBV+CNSL is aggressive and commonly exhibits infiltrative parenchymal tumor burden and poor outcome.[9] High-dose methotrexate with rituximab have been used successfully in HIV-associated EBV+CNSL.[10] However, in patients with EBV+CNSL who are undergoing iatrogenic immune suppression, drug toxicity and comorbidities are a major concern and treatment success is limited.[11,12] Additional evidence-based treatments are needed to improve the outcomes for this population.[13]

We previously reported that patients with EBV+PCNSL PTLD responded exceptionally well to an antiviral-based regimen comprising ganciclovir (GCV), zidovudine (azidothymidine [AZT]), rituximab, and dexamethasone (GARD).[11] In that study, immunohistochemistry (IHC) staining revealed the presence of EBV protein- and thymidine kinases (EBV BGLF4 and BXLF1, respectively) in CNSL biopsies. These EBV proteins are required for specific antiviral drug activation via phosphorylation of GCV and AZT from their prodrug states, thus establishing a mechanistic rationale for their therapeutic efficacy in EBV-infected cells.[14,15] The presence of BGLF4 and BXLF1 thus confers unique tumor cell vulnerabilities to GCV/AZT.[16,17] It has remained unclear if there are EBV features that indicate the presence of BGLF4/BXLF1 and could thus serve as potential biomarkers to identify tumors that will respond to GCV/AZT treatment.

In this study, we provide data on the long-term follow-up of the original GARD cohort of patients with EBV+PCNSL PTLD, in addition to new data from additional patients with EBV + CNSL (total N = 24) who represent a variety of immune suppressed states and who were treated with GARD. Using patient samples and in vitro models, we conclude that epigenetic activation and expression of *BGLF4* is present in otherwise latent EBV and thus provides a new perspective on locus-specific EBV gene control. We found that *BGLF4* DNA methylation loss is a surrogate of *BGLF4* expression and may be explored as a future biomarker for targeted CNSL treatment with the GARD regimen.

Materials and methods

Clinical data

Patients with EBV+CNSL who were treated with the GARD regimen at The Ohio State University (OSU) Wexner Medical Center between January 1998 and June 2024 were selected for this study. Clinical data were accessed retrospectively from electronic records (Tables 1 and 2). Complete response (CR), unconfirmed complete response (CRu), partial response (PR), and progressive disease (PD) were defined using guidelines from the International Primary CNS Lymphoma Collaborative Group.[18] The GARD regimen consisted of 14 days of induction treatment with IV GCV (5 mg/kg twice daily), AZT (1500 mg twice daily), and dexamethasone (10-40 mg) and 4 doses of rituximab (375 mg/m^2, days 1, 8, 15, and 22). Following induction, patients were prescribed maintenance oral valganciclovir (450 mg twice daily) and AZT (300 mg twice daily) as tolerated.

DNA and RNA isolation

Tissue biopsy DNA and RNA were isolated using the QIAamp DNA FFPE Tissue Kit (QIAGEN) and RNeasy FFPE Kit (QIAGEN), respectively, according to the manufacturers' instructions. DNA and RNA from cell culture were isolated using the QIAamp DNA Mini Kit (QIAGEN) and TRIzol reagent (Invitrogen), respectively. Plasmid and lentiviral vector DNA were prepared using the ZymoPURE Plasmid Miniprep Kit (Zymo Research) and the PureYield Plasmid Midiprep System (Promega).

Cell culture

Cells were grown in a humidified incubator at 5% CO_2 and 37°C. Hematopoietic cell lines were maintained in RPMI 1640 with 10% (v/v) fetal bovine serum, supplemented with penicillin/streptomycin and GlutaMAX (Thermo Fisher Scientific). Lymphoblastoid cell lines were generated as described.[19] HEK293 (CVCL_0045), MEC1/2 (CVCL_1870/1871), and Raji (CVCL_0511) lines were obtained from Christoph Plass's group (German Cancer Research Center); YT cells (CVCL_1797) were obtained from Bethany Mundy's group (The Ohio State University); and Lenti-X HEK293T (CVCL_0063) cells were from Takara Bio. M81 (BZLF1/BRLF1 double knockout) EBV-carrying HEK293[20] cells were a gift from

Table 1. Characteristics of the patients with CNSL

ID	Age	Sex	Race	Cause of CNSL	Primary or secondary	Reason for immunosuppression	Pathologic diagnosis	Biopsy EBER status	EBV DNA in blood	EBV DNA in CSF	Reported previously[11]	DNA methylation cohort
1	35	M	W	PTLD	Primary	Kidney transplant	Grade III LYG	Positive	None detected (<2000 copies per mL)	Detected (no viral load)	Yes	Yes
2	48	M	W	PTLD	Primary	Kidney/pancreas transplant	Grade III LYG	Positive	None detected (<2000 copies per mL)	Not tested	Yes	Yes
3	28	M	W	PTLD	Primary	Kidney transplant[a]	DLBCL	Positive	None detected (<2000 copies per mL)	Not tested	Yes	Yes
4	45	M	W	PTLD	Primary	Kidney transplant	DLBCL	Positive	Not tested	Not tested	Yes	No
5	58	M	W	PTLD	Primary	Kidney transplant	Large B-cell PTLD	Positive	Detected (1500 copies per mL)	None detected	Yes	No
6	77	F	W	PTLD	Primary	Kidney transplant	Polymorphic PTLD	Positive	None detected (<2000 copies per mL)	Detected (no viral load)	Yes	No
7	50	F	W	PTLD	Primary	Kidney transplant	DLBCL	Positive	Detected (2600 copies per mL)	Detected (555 copies per mL)	Yes	No
8	60	F	W	PTLD	Primary	Kidney transplant	DLBCL	Positive	Detected (1000 copies per mL)	Detected (500 copies per mL)	Yes	No
9	61	F	B	PTLD	Primary	Liver transplant	B-cell PTLD	EBV+ in CSF	None detected (<2000 copies per mL)	Detected (322 000 copies per mL)	Yes	No
10	42	M	W	PTLD	Primary	Kidney/pancreas transplant	Lymphohistiocytic infiltrate with monoclonal T cells	Positive	Detected (2286 copies per mL)	Detected (<10 000 copies per mL)	Yes	Yes
11	30	M	W	PTLD	Primary	Kidney transplant[a]	DLBCL	Positive	Detected (7880 copies per mL)	Detected (>10 000 copies per mL)	No	Yes
12	71	F	W	Other immunosuppression	Primary	Seronegative arthritis	Grade 3 LYG	Positive	None detected (<2000 copies per mL)	Not tested	No	No
13	69	M	W	Other immunosuppression	Secondary	Epidermolysis bullosa acquisita, HSCT, BMT for NHL	DLBCL	Positive	None detected (<2000 copies per mL)	Detected (>10 000 copies per mL)	No	Yes
14	62	M	W	Other immunosuppression	Secondary	Psoriasis (MTX)	Large cell lymphoma of ambiguous lineage	Positive	Detected (78 693 copies per mL)	Not tested	No	No
15	46	M	B	Sporadic PCNS	Primary	None	B-cell PCNS-LPD	EBV+ in CSF	Detected (1464 copies per mL)	Detected (<10 000 copies per mL)	No	Yes
16	82	F	W	Other immunosuppression	Primary	Interstitial lung disease	DLBCL	Positive	None detected (<1000 copies per mL)	Not tested	No	No
17	77	M	W	PTLD	Secondary	Kidney transplant	DLBCL	Positive	None detected (<2000 copies per mL)	Detected (<10 000 copies per mL)	No	Yes
18	73	M	W	PTLD	Primary	Kidney transplant	DLBCL	Positive	None detected (<2000 copies per mL)	Not tested	No	Yes
19	81	M	W	Other immunosuppression	Primary	Advanced age	Grade 3 LYG	Positive	None detected (<2000 copies per mL)	Not tested	No	Yes
20	54	M	Indian	Other immunosuppression	Primary	Wegner granulomatosis and anti-GBM disease	DLBCL	Positive	None detected (<2000 copies per mL)	Not tested	No	Yes
21	29	F	Indian	PTLD	Primary	Kidney transplant[a]	High-grade B-cell PTLD	Positive	Unknown (outside hospital)	Detected (47 000 copies per mL)	No	No

A total of 24 patients with CNSL who were treated at OSU with GARD are listed. EBV DNA levels were determined using a clinical diagnostic qPCR assay at the OSU Medical Center. BMT, bone marrow transplant; DLBCL, diffuse large B-cell lymphoma; EBER, EBV encoded small RNA; F, female; GBM, glomerular basement membrane; HSCT, hematopoietic stem cell transplant; LPD, lymphoproliferative disease; LYG, lymphomatoid granulomatosis; M, male; MTX, methotrexate; NHL, non-Hodgkins lymphoma; W, white.

[a]Patient experienced graft failure of intitial transplant and received a second organ transplant.

Table 1 (continued)

ID	Age	Sex	Race	Cause of CNSL	Primary or secondary	Reason for immunosuppression	Pathologic diagnosis	Biopsy EBER status	EBV DNA in blood	EBV DNA in CSF	Reported previously[11]	DNA methylation cohort
22	72	M	W	PTLD	Primary	Heart transplant	DLBCL	Positive	Detected (13 695 copies per mL)	Not tested	No	Yes
23	76	F	W	Other immunosuppression	Primary	Type 2 diabetes	Grade 3 LYG	Positive	None detected (<2000 copies per mL)	Unknown (outside hospital)	No	No
24	18	F	W	Other immunosuppression	Primary	Juvenile rheumatoid arthritis	B-cell PCNS-LPD	EBV+ in CSF	None detected (<1000 copies per mL)	Detected (<10 000 copies per mL)	No	No

A total of 24 patients with CNSL who were treated at OSU with GARD are listed. EBV DNA levels were determined using a clinical diagnostic qPCR assay at the OSU Medical Center. BMT, bone marrow transplant; DLBCL, diffuse large B-cell lymphoma; EBER, EBV encoded small RNA; F, female; GBM, glomerular basement membrane; HSCT, hematopoietic stem cell transplant; LPD, lymphoproliferative disease; LYG, lymphomatoid granulomatosis; M, male; MTX, methotrexate; NHL, non-Hodgkins lymphoma; W, white.

[a]Patient experienced graft failure of initial transplant and received a second organ transplant.

Henri-Jacques Delecluse (German Cancer Research Center). HEK293/293T cells were maintained in Dulbecco's modified Eagle medium (Gibco) with 10% (v/v) fetal bovine serum, penicillin/streptomycin, and GlutaMAX. The Burkitt lymphoma lines Kem (CVCL_7199), Mutu (CVCL_7202), and Rael (CVCL_7208) were obtained from Lisa Giulino-Roth's group (Weill Cornell Medical College). The EBV latency stage in cell lines was either determined in our own work[19] or reported previously.[20-26] Cell line authenticity was confirmed by the respective collaborators and/or commercial suppliers. All cell lines were confirmed to be mycoplasma free by using the MycoAlert Detection Kit (Lonza) every 2 weeks during experiments.

qPCR and qRT-PCR

EBV was detected in DNA samples using qPCR with Fast SYBR Green Master Mix (Applied Biosystems) and primers that amplified *EBNA1*, and the levels were normalized to the human *ACTB* locus (supplemental Table 1). RNA expression of EBV genes was assessed using quantitative reverse-transcriptase PCR (qRT-PCR). For these assays, 1 µg of total isolated RNA was reverse transcribed using Superscript IV reverse transcriptase (Invitrogen) with random hexamer oligonucleotides (QIAGEN). qPCR was carried out using primers for EBV *BZLF1*, *BXLF1*, *BGLF4*, and *LMP1*, and the levels were normalized to human *ACTB* signal (supplemental Table 1). qRT-PCR was performed using TaqMan Fast Advanced Master Mix (Applied Biosystems) and PrimeTime qPCR Probe Assays with FAM/ZEN/IBFQ probes (Integrated DNA Technologies). Samples were run in technical duplicates and only included in the analysis when both readouts yielded gene expression values within a 15% range of each other. qPCR was performed on a QuantStudio 7 Pro qPCR system (Applied Biosystems).

DNA methylation assays

DNA methylation analysis of the *LMP1*, *BGLF4*, *BXLF1*, and *BZLF1* regions (supplemental Table 1) was performed using the EpiTYPER assay as described previously.[22] DNA was bisulfite converted using the EZ DNA methylation kit (Zymo Research) and EBV regions were amplified using PCR with primers specific for bisulfite DNA (supplemental Table 1). The PCR products were analyzed using Matrix-Assisted Laser Desorption/Ionization-Time of Flight (MALDI-ToF) mass spectrometry (Agena Bioscience). The ratios of unmethylated vs methylated mass peaks were used to calculate the percentage of DNA methylation. Global EBV DNA methylation analysis was carried out using the methylation-iPLEX assay as described.[27] iPLEX capture and extension primers were designed from bisulfite-converted DNA sequences using the Typer4.0 software (Agena Bioscience; supplemental Table 1). Samples were dispensed onto 384-well SpectroCHIP arrays using the RS1000 Nanodispenser and analyzed using the MassARRAY Analyzer4 system (Agena Bioscience).

Luciferase reporter assays

Luciferase assays were carried out in reporter vector pCpGfree promoter-lucia (Invivogen) as published.[28] *BGLF4* fragments were amplified using PCR (supplemental Table 1) and cloned into HindIII/SdaI restriction sites using standard techniques. Reporter vectors were in vitro methylated using M.SssI CpG

Table 2. Treatment response and survival in patients with CNSL who received GARD

ID	Transplant induction	Immunosuppression at diagnosis	Previous treatment	Alterations to induction	Response to GARD	Additional treatment	Survival	Response at time of death	Survival time, y
1	ATG	Neoral/CellCept prednisone	None	No dex	CR	None	A	–	15.4
2	ATG	Rapamune/Myfotic	None	No dex, 1 week of 2.5 mg/kg GCV, then increased to 5 mg/kg	CRu	Repeat induction	D	CRu	11.5
3	ATG/CellCept + pheresis	Rapamune/CellCept	None	None	CR	None	A	–	14.2
4	Unk	CellCept prednisone	None	No rituximab, 2.5 mg/kg GCV	CR	None	D	CR	11.8
5	ATG	Neoral/Myfotic	None	No rituximab, 1.25 mg/kg GCV	CR	None	D	CR	3.8
6	ATG	Neoral/Myfotic	Steroids	1200 mg AZT	CRu	None	D	CRu	1.7
7	Unk	Neoral/CellCept	Rituximab WBXRT	None	CRu	None	A	–	13.3
8	ATG	CellCept/rapamune prednisone	None	Two doses of rituximab	CRu	None	D	CRu	0.3
9	Unk	Neoral/Myfotic prednisone	None	None	SD	Rituximab, IV AZT/GCV, WBXRT	D	PD	0.3
10	ATG	Myfotic, Tacrolimus	None	1200 mg AZT	CR	None	A	–	10.7
11	Unk	CellCept/rapamune Prednisone	None	None	PD	MTX, IV AZT	A	–	10.2
12	––	Methotrexate	None	None	CR	None	A	–	10.0
13	Etoposide, ARA-C, platinum	CellCept prednisone	None	IV AZT/GCV for 13 d, rituximab delayed	PR	PO AZT/GCV	D	PD	0.9
14	––	Adalimumab	RM-CHOP, brentuximab, romidepsin, BR	All treatments stopped after 1 week	PD	None	D	PD	0.05
15	––	––	None	None	CR	None	A	–	3.3
16	––	CellCept	Dex, PLEX	None	SD	None	D	SD	0.2
17	ATG	Everolimus Neoral	GARD*	None	PR	MTX, rituximab, dex	D	CR	5.4
18	ATG	Rapamune Myfotic	None	AZT stopped at 1 week	CR	None	D	CR	2.2
19	––	––	None	None	CRu	None	A	–	6.4
20	––	CellCept prednisone	None	IV medications held on days 9, 11, 12, and 13 because of mental status change and refusal	PR	Rituximab and MTX	D	CRu	1.2
21	Unk	CellCept	None	AZT PO	CRu	None	A	–	2.6
22		Neoral/CellCept prednisone	None	2.5 mg GCV, 1200 mg AZT	PD	None	D	PD	0.1
23	––	––	None	None	PR	None	D	PD	0.8
24	––	Infliximab	None	None	CR	None	A	–	5.1

A, alive; ARA-C, cytosine arabinoside or cytarabine; ATG, antithymocyte globulin; D, deceased; Dex, dexamethasone; MTX, methotrexate; PLEX, plasma exchange; PO, per oral; RB, rituximab bendamustine; RM-CHOP, rituximab methotrexate cyclophosphamide doxorubicin vincristine; Unk, unknown; WBXRT, whole brain radiation.

*Patient received GARD for a PTLD lesion in the lung.

methyltransferase (Thermo Fisher Scientific). Luciferase reporters were transfected into HEK293 cells using TransIT-LT1 reagent (Mirus Bio), and the luciferase activity was measured after 48 hours using a Synergy HT plate reader (Biotek). Data were normalized to cotransfected internal control plasmid Firefly luciferase plasmid (pGl4.10 ACTB promoter-luc2, Promega).

5'RACE

BGLF4 5' rapid amplification of complimentary DNA (cDNA) ends (5'RACE) was performed according to published protocols,[29] with modifications. For these assays, 5 µg of total RNA was reverse transcribed using the gene-specific primer (GSP), used for reverse transcription(RT) (supplemental Table 1), followed by amplification using nested PCRs with the GSP (gene specific), oligo(dT)-tailed primer (Qt), nested PCR-outer (Qo), and nested PCR-inner (Qi) primers (supplemental Table 1; Scotto-Lavino and Du[29]). The products were gel purified and cloned into pDONR221 (Invitrogen) using Gateway BP clonase II (Invitrogen), followed by Sanger sequencing at the OSU Genomics Shared Resource. The sequences were mapped to the EBV genome to determine the 5' ends as transcription start sites (TSS).

Data analysis and statistics

Statistical significance was determined using unpaired, 2-tailed *t* tests, unless stated otherwise. Unsupervised clustering was carried out using Cluster3.[30] EBV genomic data tracks were generated from an EBV reference genome (Refseq ID: NC_007605.1) using Integrative Genomics Viewer. Violin plots were generated using BoxPlotR.[31] Overall survival was defined as the time from the start of treatment until death from all causes. Patients who were alive at the last available follow-up date were censored. Time to progression was defined as the time from the start of treatment until disease progression or death from CNSL. Patients who died from other causes were censored. Treatment-related mortality (TRM) was defined as death occurring within 90 days of completion of the GARD regimen and not a consequence of progressive disease.

Ethics statement

The research was approved by the OSU institutional review board (IRB 2023C0117). Only researchers on the institutional review board application with appropriate approvals to access clinical data had access to identifiable patient information (C.W., H.L.K., and R.A.B.).

Results

Long-term follow-up reveals durable responses to GARD in EBV+CNSL

A total of 24 patients with EBV+CNSL were treated at OSU with GARD between 1998 and 2024, and a subset of these patients was previously described.[11] In this study, we report additional follow-up data on these patients and new patients with PCNSL PTLD, systemic PTLD with secondary CNS involvement, patients on iatrogenic immune suppression for autoimmune conditions, PCNSL in the setting of advanced age (>80 years old), and EBV+PCNSL with no indicators of immunosuppression (Table 1). The median age at diagnosis was 56 ± 19 years (supplemental Table 2). One patient had improvements in the lesion size after treatment but passed away from septic shock. Thus, the TRM was 4.1% (1/24). Diffuse large B-cell lymphoma was the most common histology (n = 11; 45.8%), followed by grade 3 lymphomatoid granulomatosis (n = 5; 20.8%), other B-cell lymphoproliferative disease (n = 5; 20.8%), and polymorphic diagnosis (n = 3; 12.5%; Table 1). Rapid resolution of CNSL lesions after GARD induction was observed (Figure 1A). Long-term follow up revealed durable

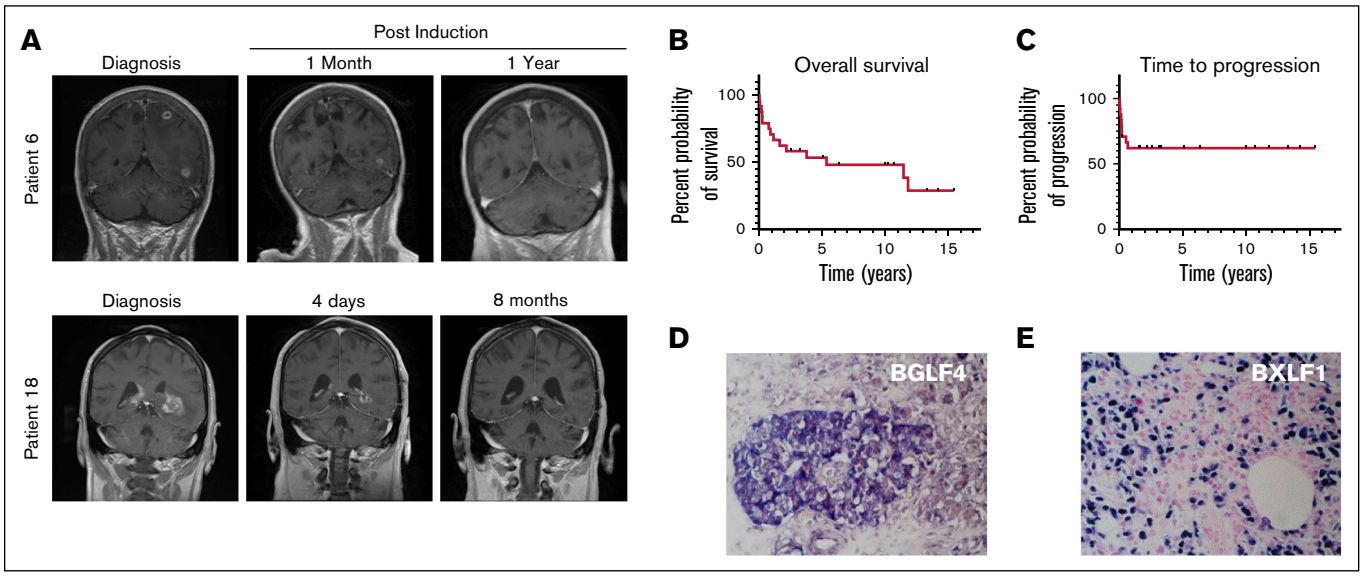

Figure 1. Clinical GARD response characteristics of EBV+CNSL. (A) Representative contrast enhanced magnetic resonance images (MRIs) from 2 patients with sequential imaging. Both patients achieved complete and durable responses. MRIs visualized and captured using NilRead software by Hyland. (B) Kaplan-Meier curves representing OS and (C) TTP in 24 patients with CNSL who were treated at OSU. (D-E) Representative IHC images of the lytic EBV proteins BXLF1 and BGLF4 from samples included in the study. IHC was performed as previously described.[11]

responses and favorable OS and TTP in patients with CNSL who were treated with GARD (Figure 1B-C). The median survival time was 5.4 years, and 15 patients (63%) achieved a CR/CRu, with an overall response rate of 79% (n = 19; Table 2). The 2-year survival was 63% (95% confidence interval [CI], 46%-85%) and 5-year survival was 53% (95% CI, 37%-78%; Figure 1B; Table 2). Primary disease showed a trend toward a superior response to GARD when compared with systemic disease (median survival, 10 years vs 11.5 years; $P = .0535$; supplemental Table 3; supplemental Figure 1A). Immunohistochemistry staining of biopsy samples from patients with primary CNSL was performed (Figure 1D-E; Dugan et al[11]) and showed BXLF1 and BGLF4 in all cases.

We compared our GARD findings with previously published studies that evaluated the survival of patients with EBV+ CNSL (supplemental Table 4).[32-36] GARD yielded a better median survival than all other studies and showed a better overall response rate than all but 1 study. Of these studies, Snanoudj et al[32] (supplemental Table 5) reported individual survival data of patients with PCNSL who underwent a renal transplant, thus enabling us to conduct a direct comparison of survival. When comparing the patients who underwent a renal transplant and who were treated with GARD (n = 13) with the Snanoudj cohort, those who were treated with GARD showed a significant survival advantage (supplemental Figure 1B; $P = .0465$). Of our GARD-treated patients who had available biopsies (n = 12), only 1 patient did not express *BGLF4*. This patient was the only patient of the 12 who experienced progressive disease following GARD therapy (patient 11; Table 2). In contrast, *BGLF4* expression was not associated with increased survival independent of GARD (N = 24 systemic PTLDs; $P = .6888$; supplemental Figure 1C).

DNA methylation loss in *BGLF4* is associated with *BGLF4* expression in CNSL

We have reported the expression of BGLF4 and BXLF1 in EBV+CNSL.[11] However, it remained uncertain if the presence of BXLF1/BGLF4 was a consequence of lytic EBV replication. To address this, we performed gene expression analysis of lytic and latent EBV transcripts in EBV + CNSL tumor tissue biopsies (n = 12; Table 1) and patients with systemic EBV+ PTLD who were not treated with GARD (n = 24). Patients with EBV + CNSL showed higher *BGLF4* expression levels than those with systemic PTLDs (Figure 2A), and the *BXLF1* expression differences neared statistical significance (supplemental Figure 2A). RNA expression of the lytic transcripts *BZLF1*, *BRLF1*, and *BMRF1* (supplemental Figure 2B-D), all indicators of lytic cycle entry,[2] was low or undetectable in many systemic PTLDs and was consistently detectable in only 1 EBV+CNSL case (1/12, 8%) and only at low levels (supplemental Table 6/supplemental Figure 2, marked †). RNA expression of the EBV latent membrane protein 1 (*LMP1*; supplemental Figure 2E) was detectable in most systemic PTLDs (16/21, 73%) and CNSLs (9/12, 75%), indicating a latency type 2/3 EBV state.

To distinguish the specific epigenetic state of the EBV loci, we subsequently performed quantitative DNA methylation profiling of

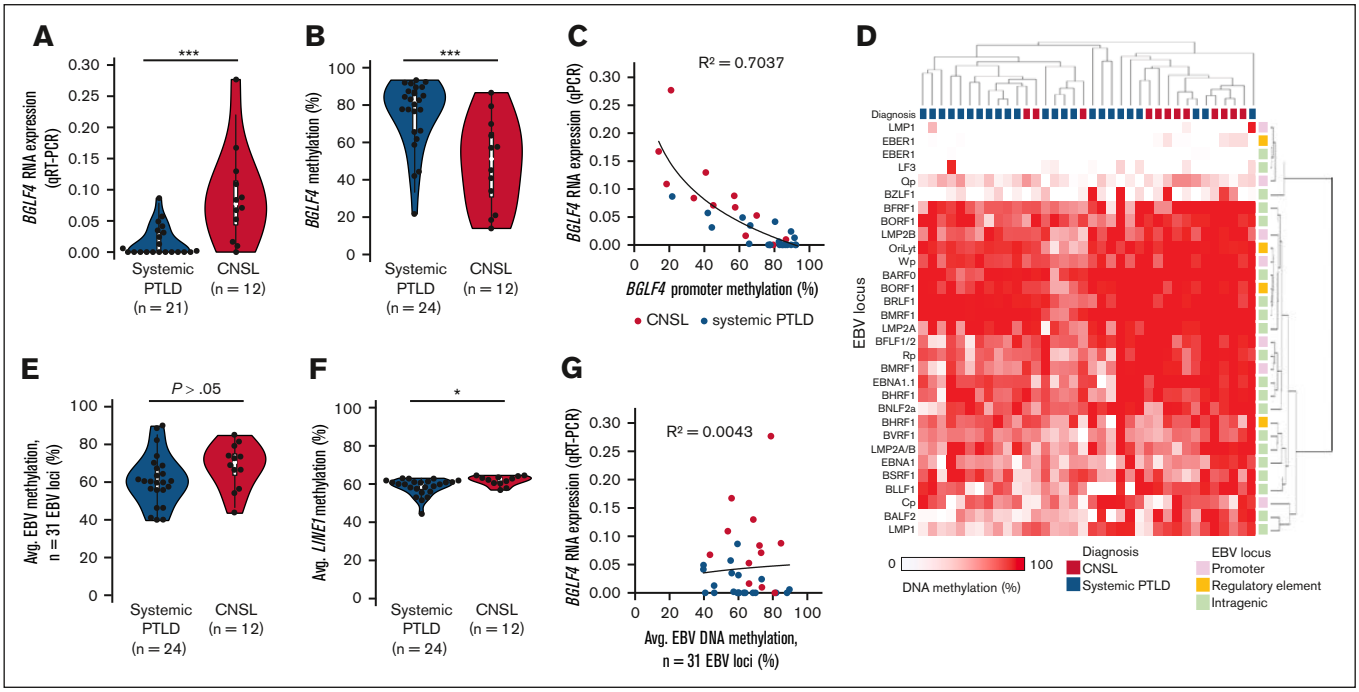

Figure 2. Lower EBV *BGLF4* DNA methylation correlates with increased *BGLF4* expression in CNSL. (A) RNA expression (qRT-PCR) and (B) EBV *BGLF4* DNA methylation determined using EpiTYPER in systemic PTLD and CNSL tissue biopsies. (C) correlation between *BGLF4* RNA expression and DNA methylation. (D) Heat map depicting EBV DNA methylation of 31 methylation sites, determined using the methylation iPLEX assay, arranged using unsupervised clustering and annotated based on sample cohort and EBV locus.[3] DNA methylation is depicted from 0% methylated (white) to 100% methylated (red). (E) Average EBV DNA methylation determined using the iPLEX assay. (F) Average *LINE1* DNA methylation, determined using EpiTYPER. (G) Correlation of *BGLF4* RNA expression and average EBV DNA methylation from panel D. R^2, correlation coefficient. *$P < .05$; ***$P < .001$, *t* test (panels B,E,F, exact Wilcoxon-Mann-Whitney test).

the *BGLF4*, *BXLF1*, *BZLF1*, *BRLF1*, *BMRF1*, and *LMP1* upstream sequences using the EpiTYPER assay[37] in tissue biopsy DNA. We revealed significantly lower *BGLF4* methylation in CNSL cases than in systemic PTLD cases ($P = .0006$; Figure 2B), but there were no significant differences in *BXLF1*, *BZLF1*, *BRLF1*, *BMRF1*, or *LMP1* (supplemental Figure 2F-J). A comparison of the RNA expression and methylation showed an inverse correlation for *BGLF4* (Figure 2C).

To determine whether the *BGLF4* methylation differences between EBV + CNSL cases and systemic PTLD cases were the consequence of global methylation alterations, we evaluated 31 CpG methylation sites evenly distributed across the EBV genome (Figure 2D-E). We also evaluated human genomic *LINE1*, *LTR*, and *Alu* repeat element methylation as a surrogate of global host cellular methylation (Figure 2F; supplemental Figure 2K-L). With the exception of a low (average, 3.2%) methylation difference in *LINE1*, the global EBV and host cellular DNA methylation levels were not significantly different between the EBV + CNSL cases and the systemic PTLD cases, thus indicating a localized DNA methylation loss at *BGLF4*. We found no significant correlation between the *BGLF4* RNA expression and average EBV methylation (Figure 2G). It is known that lytic EBV activation exhibits a rapid expansion of EBV DNA copies, a loss of global EBV DNA methylation,[2] and widespread lytic RNA expression, including *BGLF4*.[38] We assessed these lytic EBV characteristics by correlating *BGLF4* expression with EBV DNA loads in tissue samples (supplemental Figure 2M), clinically determined EBV qPCR data from serum samples (supplemental Figure 2N), and overall EBV methylation vs EBV load (supplemental Figure 2O). These comparisons showed no evident correlations. Taken together, the strikingly low DNA methylation at *BGLF4* in EBV+CNSL cases did not align with correlates of lytic virus activity, indicating a highly localized methylation loss. EBV+CNSL cases retained features of viral latency, such as elevated global DNA methylation (Figure 2D-E), latent gene expression (supplemental Figure 2E), and a lack of the critical lytic transcripts *BZLF1*, *BRLF1*, and *BMRF1* (supplemental Figure 2B-D).

Low DNA methylation at 3 individual *BGLF4* upstream loci

To understand the reach of lowered methylation in EBV+CNSL, we carried out a detailed assessment of DNA methylation in the 1 kilobase upstream region of *BGLF4* that was previously shown to hold the TSS.[39] Using the EpiTYPER assay, we derived quantitative, single CpG resolution methylation maps for our CNSL and systemic PTLD biopsies (Figure 3A; supplemental Figure 3). A significant methylation reduction in CNSL was localized to 3 differentially methylated regions (DMRs), and each DMR had at least 1 single informative CpG dinucleotide with pronounced methylation loss in CNSL (CpG1/2/3; Figure 3B). Localized *BGLF4* methylation loss was also observed in a subset of systemic PTLD cases (Figure 3B; supplemental Figure 3; supplemental Data 1), and more than one-third (9/24; 38%) had at least 1 DMR with a methylation level below 50%. A comparison of the histologic subtypes in CNSL and systemic PTLDs revealed that significant methylation differences were retained at the *BGLF4* CpG sites when CNS and systemic DLBCLs (including grade 3 lymphomatoid granulomatosis) were compared (supplemental Figure 4A-C). All 3 informative DMR CpG sites displayed an inverse correlation with *BGLF4* RNA expression (Figure 3C-E). When categorizing PTLD tissue samples based on the number of hypomethylated (<50% methylation) informative CpGs, we found that *BGLF4* RNA expression increased with the number hypomethylated CpG sites (Figure 3F). The presence of 2 or more informative DMR CpGs with <50% methylation indicated high (fourth quartile) *BGLF4* expression with high sensitivity and specificity (supplemental Figure 4D). As a proof of concept, we determined EBV *BGLF4* methylation in cerebrospinal fluid (CSF) samples from 2 patients with EBV-driven DLBCL and CNS involvement and EBV encephalitis caused by EBV reactivation, respectively. We found significantly lower *BGLF4* methylation in the viral reactivation setting, distinguishing it from EBV-driven malignancy (supplemental Figure 4E-F). In summary, we found that highly localized methylation reduction was associated with *BGLF4* expression.

BGLF4 DMRs have gene promoter activity and mark 3 distinct *BGLF4* transcription start sites

The identification of 3 DMRs pointed to the presence of *BGLF4* gene regulatory elements. We tested the functional properties of the *BGLF4* upstream elements in a dual luciferase reporter assay and found that all 3 DMR regions carried gene promoter activity significantly above that of a control minimal promoter (Figure 4A). These activities were frequently increased when a HEK293 model that carried latent EBV was used (supplemental Figure 5A). Using in vitro CpG-methylated reporter constructs, we revealed that DNA methylation significantly decreased the promoter activity (Figure 4B). To identify whether the observed regions of promoter activity gave rise to RNA transcription, we carried out 5'RACE. Using amplification of cDNA that ranged from the *BGLF4* start codon to upstream sequences, we identified 3 distinct *BGLF4* TSSs within DMR2 and DMR3 in 5 primary CNSL samples (Figure 4C-G) and 4 EBV cell models (supplemental Figure 5B-E; supplemental Table 7). Combining data from our EBV cell models and CNSL biopsies, we showed that TSS activity was strongly associated with CpG methylation immediately adjacent to each TSS (Figure 4H). This association was confirmed in all 3 TSS sites individually (supplemental Figure 5F), including methylation in a 25-bp window around the TSS (supplemental Figure 5G). Together, our data revealed promoter activity in *BGLF4* upstream DMR elements that give rise to distinct viral *BGLF4* transcripts in CNSL.

TET2 is required for the establishment of decreased *BGLF4* DMR methylation and *BGLF4* expression

We next sought to determine the epigenetic factors that establish the *BGLF4* DNA methylation patterns. Targeted loss of DNA methylation in the human genome is mediated by the ten-eleven translocation (TET) DNA demethylases.[40] TET2 has been reported to affect EBV latency and gene expression.[41,42] To test whether TET2 may be required for methylation regulation at *BGLF4*, we implemented a model that recapitulates the establishment of *BGLF4* DNA methylation patterns on EBV following host cell infection and latency establishment. We assessed our cell line data (supplemental Figure 3A) and found that 5 cell lines (Raji, Rael, MEC1, Kem, HEK293) carried elevated *BGLF4* DNA methylation levels that resembled the systemic PTLD samples. HEK293 cells displayed pronounced localized methylation

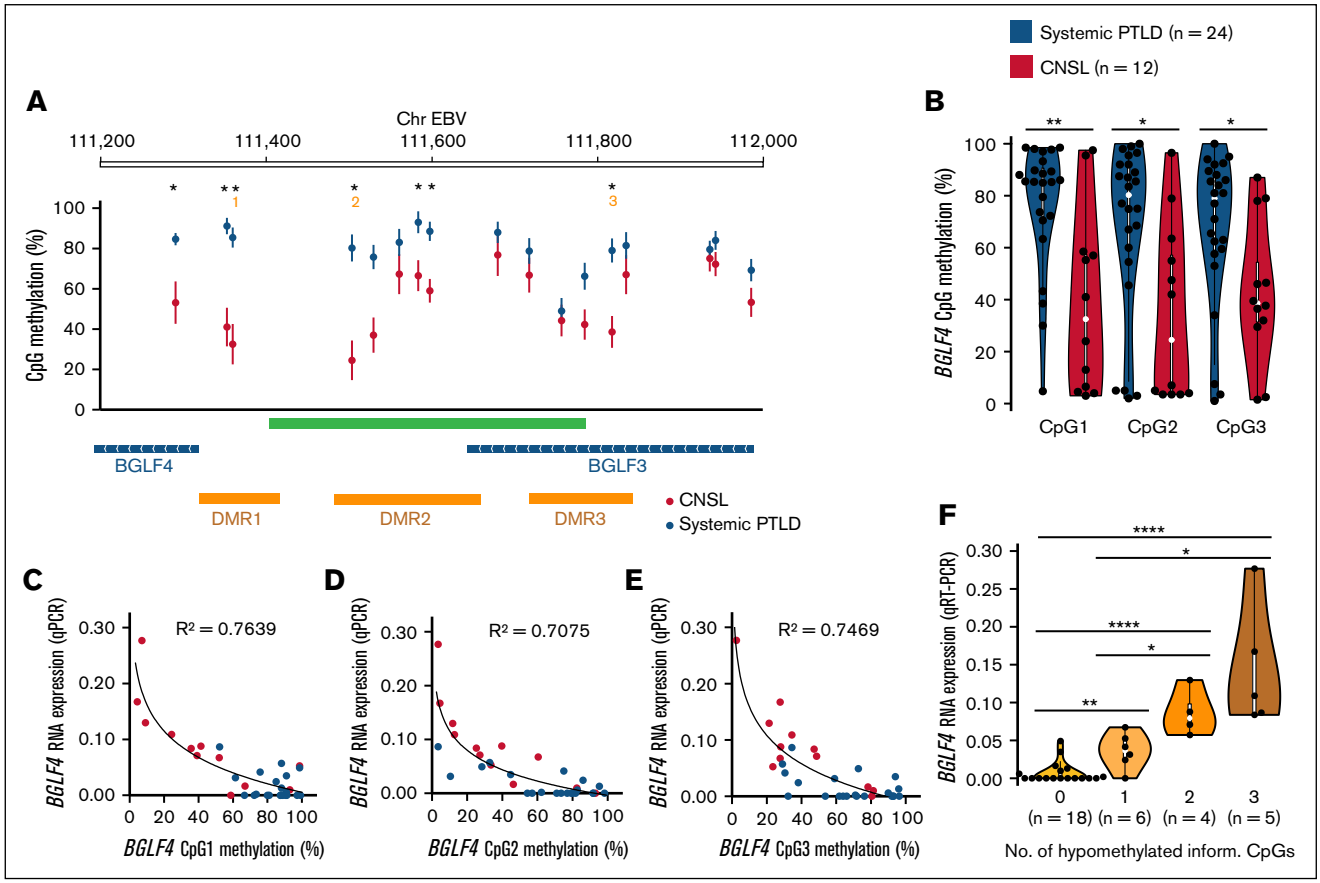

Figure 3. Localized methylation loss at EBV *BGLF4*. (A) Expanded methylation analysis of the *BGLF4* upstream locus using the EpiTYPER assay. EBV genomic coordinates and statistical significance for individual CpG sites are annotated above. The data are shown as the mean ± standard error of the mean DNA methylation in the PCNSL (n = 12) and systemic PTLDs (N = 24) cohorts. Lower panel: the CpG islands (green), EBV transcripts (blue), and DMRs (orange) are annotated. (B) DNA methylation at 3 individual DMR CpG sites marked in panel A. (C-E) Correlation between DNA methylation and *BGLF4* RNA expression at 3 DMR CpG sites of the *BGLF4* upstream locus. (F) Classification of *BGLF4* methylation based on the number of DMR CpG sites with reduced methylation levels and the corresponding *BGLF4* RNA expression levels. **P* < .05; ***P* < .01; *****P* < .0001, *t* test (panels A-B, exact Wilcoxon-Mann-Whitney test).

patterns at *BGLF4* with DMR3 having greatly lowered methylation, accompanied by specific transcription from that locus (supplemental Figure 5B). The HEK293 EBV model further bypasses the disruption of viral latency through a BZLF1/BRLF1 gene knockout,[23] thereby enabling an investigation of *BGLF4* strictly outside of lytic activation. We therefore established a model of latency/DNA methylation establishment using this cell line (supplemental Figure 6A; Tsai et al[23]) and investigated biallelic CRISPR knockout of *TET2* (*TET2*$^{-/-}$; supplemental Figure 6B). A comparison of EBV infection in control or TET2$^{-/-}$ cells (Figure 5A) revealed that DMR3 near the active *BGLF4* TSS significantly gained DNA methylation (Figure 5B), accompanied by significantly decreased *BGLF4* RNA expression (Figure 5C). We found that *TET2* knockout did not significantly alter the global EBV methylation (Figure 5D-E). We validated these findings in a second model of TET deficiency that relied on the overexpression of mutant isocitrate dehydrogenase 1 (IDH1, R132H), which impairs all 3 TET family members by generating α-hydroxyglutarate[43] to target enzymatic activity directly. We found that lentiviral overexpression of IDH1 R132H (supplemental Figure 6C), as well as TET2$^{-/-}$ cells, had greatly reduced overall hydroxymethylcytosine (5-hmC) and 5-mC hydroxylase enzymatic activity (supplemental Figure 6D-E). After EBV M81 infection, HEK293 cells with IDH1 R132H again had elevated DNA methylation and lowered RNA expression levels at *BGLF4* (supplemental Figure 6F-H). IDH1 R132H expression also led to a modest but significant increase in global EBV methylation (supplemental Figure 6I-J). Taken together, we employed 2 distinct models of TET deficiency and found that locus-specific lack of methylation at *BGLF4* requires TET2.

Discussion

EBV-associated lymphomas are believed to be strictly latent with silencing of most EBV genes, including *BGLF4*. Previous research has focused on interventions that reactivate EBV and make it vulnerable to antiviral treatments or immune detection.[22,44] Here, we provide evidence that the antiviral regimen GARD has efficacy in EBV-associated CNSL. An assessment of multiple surrogate markers of lytic EBV activity in CNSL suggested that full lytic EBV reactivation may not be required for GARD's efficacy, but expression of the viral kinase BGLF4 may be associated with response to GARD. Only 1 patient had progressive disease with

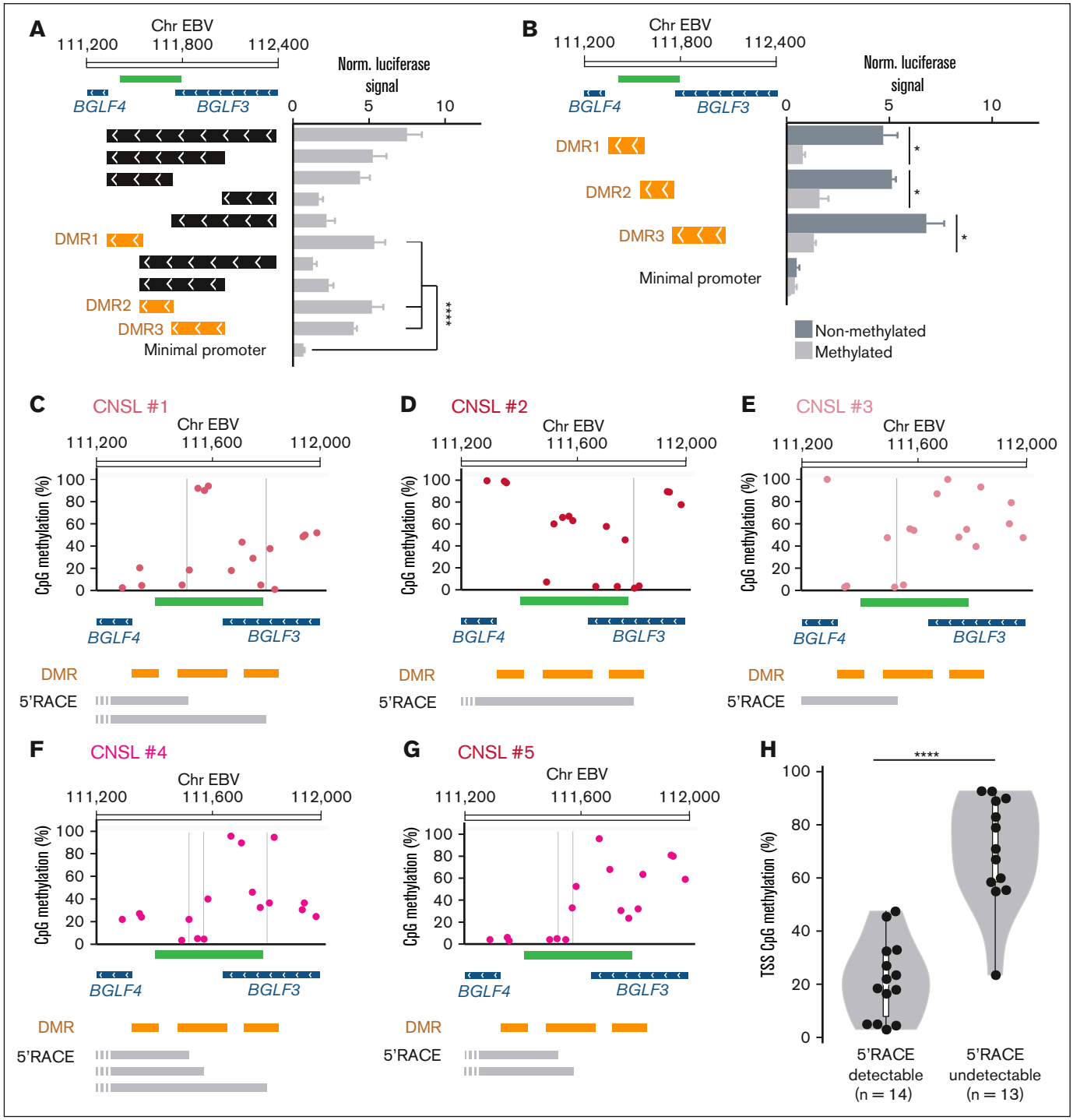

Figure 4. *BGLF4* DMRs possess gene promoter activity. (A-B) Luciferase reporter assay of *BGLF4* upstream DNA elements alone (A) or after in vitro DNA methylation or reporter constructs (B). Bar graphs show the mean ± standard deviation of quadruplicate readouts in HEK293 cells. The arrows indicate the reporter element orientation in reference to the EBV genome. (C-G) Results of the 5'RACE in 5 PCNSL samples with high levels of *BGLF4* RNA expression. The plots show DNA methylation across the *BGLF4* upstream region in each sample with the detected TSS marked by vertical lines. Lower panels: sequenced transcripts from 5'RACE (gray). DNA sequences representing DMRs (orange), EBV genomic coordinates, CpG islands (green), and EBV transcripts (blue) are indicated. (H) Violin plot depicting DNA methylation at CpG sites closest to the TSS with either detectable (n = 14) or undetectable (n = 13) transcript. Data are aggregate readouts of 5 PCNSL samples from (C-G) and an additional 4 EBV+ cell lines (supplemental Figure 5B-E). *$P < .05$; ****$P < .0001$, *t* test (panel H, exact Wilcoxon-Mann-Whitney test).

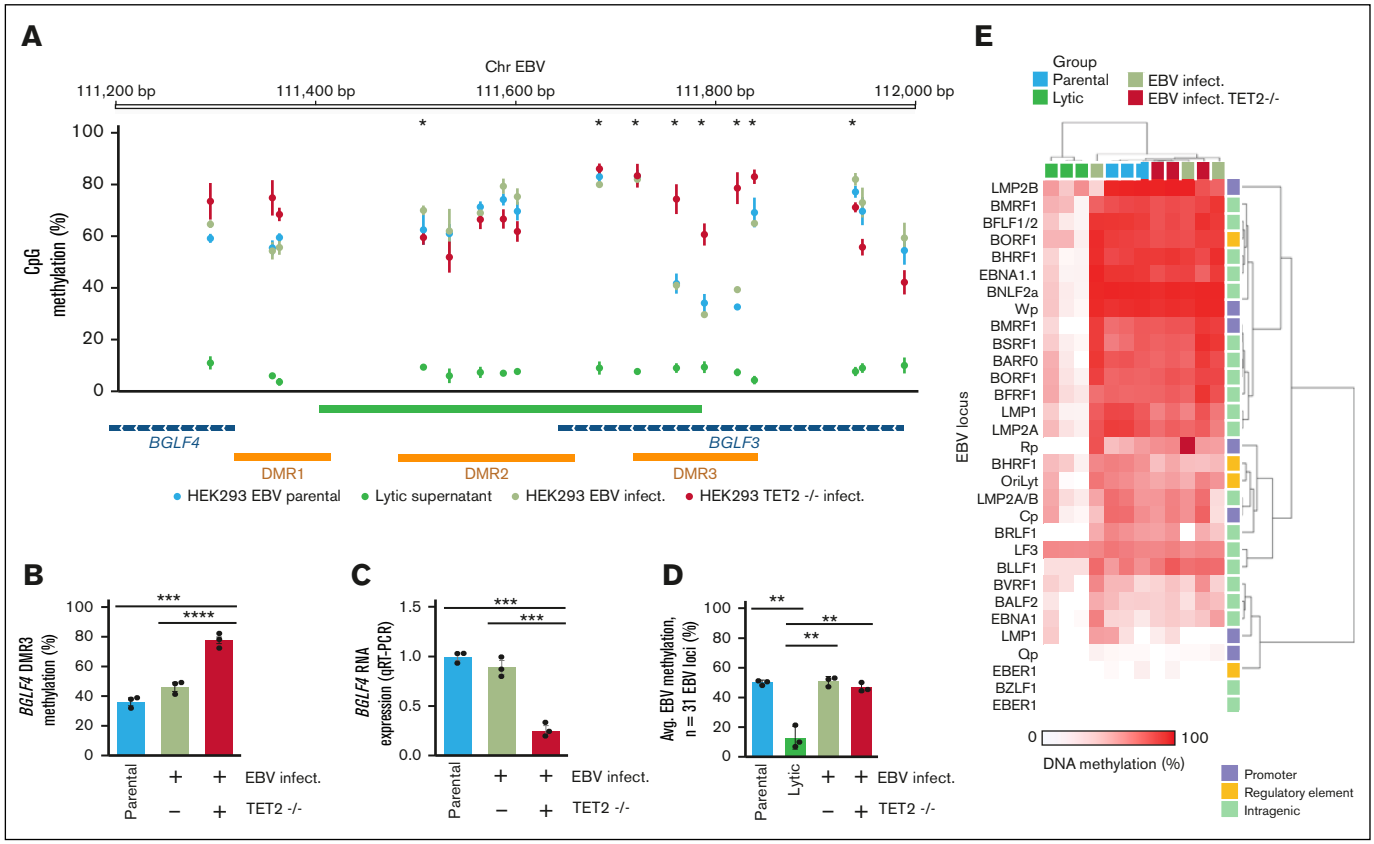

Figure 5. TET2 knockout increases *BGLF4* promoter DNA methylation and lowers *BGLF4* expression. (A) Methylation analysis of the *BGLF4* upstream locus using the EpiTYPER assay in M81 EBV HEK293 cells. The EBV genomic coordinates and statistical significance for individual CpG sites are annotated above. Lower panel: CpG islands (green), EBV transcripts (blue), and DMRs (orange) are annotated. (B-C) *BGLF4* DNA methylation average from the DMR3 CpG sites (B; ChrEBV:111757, 111785, 111818) and *BGLF4* RNA expression (C) in parental, wild-type reinfected control or TET2$^{-/-}$ reinfected HEK293 cells. (D) EBV DNA methylation average of 31 EBV CpG sites, determined using the iPLEX assay in parental, lytic-induced, reinfected, or TET2$^{-/-}$ reinfected HEK293 cells. (E) Heat map depicting EBV DNA methylation of 31 methylation sites, determined using the methylation iPLEX assay in parental M81 EBV HEK293 (blue), after lytic induction (green), EBV-infected HEK293 wild type control (brown) or TET2$^{-/-}$ (red) cells. Samples were arranged using unsupervised clustering and annotated based on the sample cohort and EBV locus. DNA methylation in the heat maps is depicted from 0% (white) to 100% methylated (red). All data are presented as the mean ± standard deviation of biologic triplicates. *$P < .05$; **$P < .01$; ***$P < .001$; ****$P < .0001$, *t* test (panel A, exact Wilcoxon-Mann-Whitney test).

GARD treatment (Table 2, patient 11), and this patient had the highest *BGLF4* methylation level (supplemental Figure 3; 84%) and was the only patient with CNSL to not express *BGLF4* (supplemental Table 6). Our study's small sample size prohibited us from determining if *BGLF4* expression was associated with a response to GARD specifically. In systemic PTLDs, *BGLF4* expression was not associated with outcomes (supplemental Figure 1C), likely because of the high variation in antiviral drug use and disease heterogeneity.

In our CNSL cohort, GARD maintained excellent overall efficacy and a low toxicity profile. The only treatment modality that seemed to surpass GARD was whole brain radiation (supplemental Table 4), but this treatment had significant toxicities and a TRM of 14% as opposed to 4.1% associated with GARD treatment. GARD treatment produced a better median survival than observed in other comparable studies.[32-36] Drawing direct comparisons between the studies is limited by a lack of standardized treatment and the rarity of CNSL. However, GARD showed a strong trend toward improved outcomes with the added advantage of offering a standardized treatment option with low toxicity for EBV+CNSL. GARD is especially attractive for patients with organ allografts who are at high risk for toxicity and who would not be good candidates for high-dose methotrexate-based regimens. The development of treatment options for this patient population remains an important unmet because modern treatments, such as the MATRix (methotrexate, cytarabine, thiotepa, and reituximab) regimen, have focused on immunocompetent patients with CNSL and excluded patients who were immunocompromised or of advanced age.[45]

EBV lytic activity has historically been considered a switch-like process.[2] It has remained unclear how partial EBV activation (abortive lytic cycle[46]) is achieved. Early findings on the expression of *BGLF4* indicated that *BGLF4* production required viral DNA replication and thus passive EBV DNA methylation loss.[47] However, *BGLF4* was subsequently shown to be expressed independently of viral replication,[38] and we suggest that a loss of *BGLF4* DNA methylation in this setting may be carried out actively by TET2. We report experimental evidence that *BGLF4* undergoes locus-specific epigenetic activation through DNA methylation loss

rather than being part of a global lytic activation program. This was supported by our HEK293 model in which knockout of the lytic *BZLF1/BRLF1* genes excluded EBV lytic activation although *BGLF4* expression was still observed.

We established that TET2 is required for large parts of *BGLF4* expression. TET2 has been shown to have crucial functions in EBV genomic activity.[41,42,48] We expand on these findings by establishing the specific requirement of TET2 for the *BGLF4* methylation decrease. Of note, TET2 and IDH1/2 mutations are enriched in EBV-associated lymphomas.[49] We propose that such mutations may hold significance for EBV's biologic state and may be affecting *BGLF4* expression. P53 has also shown function in EBV activity with studies suggesting that p53 can contribute to lytic reactivation and that several EBV proteins repress p53.[50-52] Although EBV-associated CNSL is enriched in mutations of epigenetic regulators, it exhibits an overall diminished mutational burden when compared with EBV-negative CNSL and lacks recurrent mutations like *CDKN2A*, a regulator of p53.[8,49] Given the importance and heterogeneity of the p53 pathway in EBV activity, it is tempting to speculate that p53 may be involved in locus-specific activation of genes like *BGFL4*.

Clinical EBV detection is mostly limited to qPCR, but a high tumor load in EBV^+ malignancies can mimic high viral loads associated with lytic activation, making these 2 states indistinguishable when using qPCR.[5,6] Even in the absence of malignancy, ~20% of high-risk individuals show detectable EBV in the CNS.[53] We lay out how EBV methylation can be leveraged to add context to the DNA load and aid in characterizing EBV-associated diseases. In EBV+CNSL, EBV is frequently detectable in the CSF, offering a minimally invasive way to detect EBV from CSF DNA.[5] We identified key methylation sites associated with *BGLF4* expression and proved that their detection is possible in CSF (supplemental Figure 4E-F). We propose these sites as potential indicators for patients to respond to GARD. In the future, this may offer an opportunity to screen for nonmethylated *BGLF4* and initiate targeted antiviral treatment of EBV+CNSL.

Acknowledgments

The authors thank The Ohio State University (OSU) Tissue Archive Services for sample procurement and distribution, and Matthew Purcell for assisting with cell sorting.

This work was supported by funding from OSU P30 Cancer Center Support Grant (NCI P30CA016058). C.W. and C.C.O. received funding support from the American Cancer Society grant RSG-21-150-01-CDP. H.L.K. was supported by the American Society of Hematology Medical Student Physician-Scientist Award and an National Cancer Institute F30 fellowship grant (1F30CA306400-01A1).

Authorship

Contribution: C.W. and H.L.K. contributed to all aspects of this publication; F.T. analyzed data and performed the statistical analyses; S.A. and S.S. performed the research and collected data; B.P. performed the research and contributed analytical tools; J.P.D. and B.M.H. performed and designed the research and collected data; M.L. and P.P. identified patients and collected data; L.V. and T.V. analyzed and interpreted data; R.F.A., S.C.K., J.F., and H.-J.D. provided reagents; M.L., L.A., G.B., and C.C.O. analyzed and interpreted data; R.A.B. designed the research and analyzed and interpreted data; C.W., H.L.K., and R.A.B. wrote the manuscript; and all authors contributed to editing and revisions.

Conflict-of-interest disclosure: The authors declare no competing financial interests.

ORCID profiles: H.L.K., 0000-0003-0885-0029; B.P., 0000-0001-8629-3454; L.V., 0000-0001-7179-9460; P.P., 0000-0002-8056-023X; T.V., 0000-0001-7603-6454; R.F.A., 0000-0003-4027-3073; J.F., 0000-0003-1620-1731; C.C.O., 0000-0001-8000-9694; R.A.B., 0000-0002-1619-4853.

Correspondence: Robert A. Baiocchi, Division of Hematology, Department of Internal Medicine, The Ohio State University, 400 West 12th Ave, Columbus, OH 43210; email: email: robert.baiocchi@osumc.edu.

References

1. Damania B, Kenney SC, Raab-Traub N. Epstein-Barr virus: biology and clinical disease. *Cell*. 2022;185(20):3652-3670.
2. Buschle A, Hammerschmidt W. Epigenetic lifestyle of Epstein-Barr virus. *Semin Immunopathol*. 2020;42(2):131-142.
3. Arvey A, Tempera I, Tsai K, et al. An atlas of the Epstein-Barr virus transcriptome and epigenome reveals host-virus regulatory interactions. *Cell Host Microbe*. 2012;12(2):233-245.
4. Woellmer A, Hammerschmidt W. Epstein-Barr virus and host cell methylation: regulation of latency, replication and virus reactivation. *Curr Opin Virol*. 2013;3(3):260-265.
5. Wang Y, Yang J, Wen Y. Lessons from Epstein-Barr virus DNA detection in cerebrospinal fluid as a diagnostic tool for EBV-induced central nervous system dysfunction among HIV-positive patients. *Biomed Pharmacother*. 2022;145:112392.
6. Bakker NA, van Imhoff GW, Verschuuren EA, van Son WJ. Presentation and early detection of post-transplant lymphoproliferative disorder after solid organ transplantation. *Transpl Int*. 2007;20(3):207-218.
7. White ML, Moore DW, Zhang Y, Mark KD, Greiner TC, Bierman PJ. Primary central nervous system post-transplant lymphoproliferative disorders: the spectrum of imaging appearances and differential. *Insights Imaging*. 2019;10(1):46.
8. Gandhi MK, Hoang T, Law SC, et al. EBV-associated primary CNS lymphoma occurring after immunosuppression is a distinct immunobiological entity. *Blood*. 2021;137(11):1468-1477.
9. Andersen O, Ernberg I, Hedström AK. Treatment options for Epstein-Barr virus-related disorders of the central nervous system. *Infect Drug Resist*. 2023;16:4599-4620.

10. Lurain K, Uldrick TS, Ramaswami R, et al. Treatment of HIV-associated primary CNS lymphoma with antiretroviral therapy, rituximab, and high-dose methotrexate. *Blood*. 2020;136(19):2229-2232.

11. Dugan JP, Haverkos BM, Villagomez L, et al. Complete and durable responses in primary central nervous system posttransplant lymphoproliferative disorder with zidovudine, ganciclovir, rituximab, and dexamethasone. *Clin Cancer Res*. 2018;24(14):3273-3281.

12. Grommes C, DeAngelis LM. Primary CNS Lymphoma. *J Clin Oncol*. 2017;35(21):2410-2418.

13. Markouli M, Ullah F, Omar N, et al. Recent advances in adult post-transplant lymphoproliferative disorder. *Cancers (Basel)*. 2022;14(23):5949.

14. Meng Q, Hagemeier SR, Fingeroth JD, Gershburg E, Pagano JS, Kenney SC. The Epstein-Barr virus (EBV)-encoded protein kinase, EBV-PK, but not the thymidine kinase (EBV-TK), is required for ganciclovir and acyclovir inhibition of lytic viral production. *J Virol*. 2010;84(9):4534-4542.

15. Gustafson EA, Chillemi AC, Sage DR, Fingeroth JD. The Epstein-Barr virus thymidine kinase does not phosphorylate ganciclovir or acyclovir and demonstrates a narrow substrate specificity compared to the herpes simplex virus type 1 thymidine kinase. *Antimicrob Agents Chemother*. 1998; 42(11):2923-2931.

16. Bayraktar UD, Diaz LA, Ashlock B, et al. Zidovudine-based lytic-inducing chemotherapy for Epstein-Barr virus-related lymphomas. *Leuk Lymphoma*. 2014;55(4):786-794.

17. Haverkos B, Alpdogan O, Baiocchi R, et al. Targeted therapy with nanatinostat and valganciclovir in recurrent EBV-positive lymphoid malignancies: a phase 1b/2 study. *Blood Adv*. 2023;7(20):6339-6350.

18. Abrey LE, Batchelor TT, Ferreri AJM, et al. Report of an international workshop to standardize baseline evaluation and response criteria for primary CNS lymphoma. *J Clin Oncol*. 2005;23(22):5034-5043.

19. Ahmed EH, Lustberg M, Hale C, et al. Follicular helper and regulatory T cells drive the development of spontaneous Epstein-Barr virus lymphoproliferative disorder. *Cancers (Basel)*. 2023;15(11):3046.

20. Tsai MH, Lin X, Shumilov A, et al. The biological properties of different Epstein-Barr virus strains explain their association with various types of cancers. *Oncotarget*. 2017;8(6):10238-10254.

21. Rasul E, Salamon D, Nagy N, et al. The MEC1 and MEC2 lines represent two CLL subclones in different stages of progression towards prolymphocytic leukemia. *PLoS One*. 2014;9(8):e106008.

22. Dalton T, Doubrovina E, Pankov D, et al. Epigenetic reprogramming sensitizes immunologically silent EBV+ lymphomas to virus-directed immunotherapy. *Blood*. 2020;135(21):1870-1881.

23. Tsai MH, Raykova A, Klinke O, et al. Spontaneous lytic replication and epitheliotropism define an Epstein-Barr virus strain found in carcinomas. *Cell Rep*. 2013;5(2):458-470.

24. Yoneda N, Tatsumi E, Kawano S, et al. Detection of Epstein-Barr virus genome in natural-killer-like cell line, YT. *Leukemia*. 1992;6(2):136-141.

25. Kanegane H, Wang F, Tosato G. Virus-cell interactions in a natural killer-like cell line from a patient with lymphoblastic lymphoma. *Blood*. 1996;88(12): 4667-4675.

26. Murata T, Noda C, Narita Y, et al. Induction of Epstein-Barr virus oncoprotein lmp1 by transcription factors AP-2 and early B cell Factor. *J Virol*. 2016; 90(8):3873-3889.

27. Giacopelli B, Zhao Q, Ruppert AS, et al. Developmental subtypes assessed by DNA methylation-iPLEX forecast the natural history of chronic lymphocytic leukemia. *Blood*. 2019;134(8):688-698.

28. Weigel C, Veldwijk MR, Oakes CC, et al. Epigenetic regulation of diacylglycerol kinase alpha promotes radiation-induced fibrosis. *Nat Commun*. 2016;7:10893.

29. Scotto-Lavino E, Du G, Frohman MA. 5' end cDNA amplification using classic RACE. *Nat Protoc*. 2006;1(6):2555-2562.

30. de Hoon MJ, Imoto S, Nolan J, Miyano S. Open source clustering software. *Bioinformatics*. 2004;20(9):1453-1454.

31. Spitzer M, Wildenhain J, Rappsilber J, Tyers M. BoxPlotR: a web tool for generation of box plots. *Nat Methods*. 2014;11(2):121-122.

32. Snanoudj R, Durrbach A, Leblond V, et al. Primary brain lymphomas after kidney transplantation: presentation and outcome. *Transplantation*. 2003; 76(6):930-937.

33. Cavaliere R, Petroni G, Lopes MB, Schiff D; International Primary Central Nervous System Lymphoma Collaborative Group. Primary central nervous system post-transplantation lymphoproliferative disorder: an international primary central nervous system lymphoma collaborative group report. *Cancer*. 2010;116(4):863-870.

34. Evens AM, Choquet S, Kroll-Desrosiers AR, et al. Primary CNS posttransplant lymphoproliferative disease (PTLD): an international report of 84 cases in the modern era. *Am J Transplant*. 2013;13(6):1512-1522.

35. Zimmermann H, Nitsche M, Pott C, et al. Reduction of immunosuppression combined with whole-brain radiotherapy and concurrent systemic rituximab is an effective yet toxic treatment of primary central nervous system post-transplant lymphoproliferative disorder (pCNS-PTLD): 14 cases from the prospective German PTLD registry. *Ann Hematol*. 2021;100(8):2043-2050.

36. Agrawal P, David KA, Chen Z, et al. EBV-positive PCNSL in older patients: incidence, characteristics, tumor pathology, and outcomes across a large multicenter cohort. *Leuk Lymphoma*. 2023;64(5):1026-1034.

37. Ehrich M, Nelson MR, Stanssens P, et al. Quantitative high-throughput analysis of DNA methylation patterns by base-specific cleavage and mass spectrometry. *Proc Natl Acad Sci U S A*. 2005;102(44):15785-15790.

38. Djavadian R, Hayes M, Johannsen E. CAGE-seq analysis of Epstein-Barr virus lytic gene transcription: 3 kinetic classes from 2 mechanisms. *PLoS Pathog*. 2018;14(6):e1007114.

39. Wang JT, Chuang YC, Chen KL, et al. Characterization of Epstein-Barr virus BGLF4 kinase expression control at the transcriptional and translational levels. *J Gen Virol*. 2010;91(Pt 9):2186-2196.

40. Verma N, Pan H, Doré LC, et al. TET proteins safeguard bivalent promoters from de novo methylation in human embryonic stem cells. *Nat Genet*. 2018;50(1):83-95.

41. Wille CK, Li Y, Rui L, Johannsen EC, Kenney SC. Restricted TET2 expression in germinal center type b cells promotes stringent epstein-barr virus latency. *J Virol*. 2017;91(5):e01987-16.

42. Lu F, Wiedmer A, Martin KA, Wickramasinghe P, Kossenkov AV, Lieberman PM. Coordinate regulation of TET2 and EBNA2 controls the DNA methylation state of latent Epstein-Barr virus. *J Virol*. 2017;91(20):e00804-17.

43. Cairns RA, Mak TW. Oncogenic isocitrate dehydrogenase mutations: mechanisms, models, and clinical opportunities. *Cancer Discov*. 2013;3(7):730-741.

44. Roychowdhury S, Peng R, Baiocchi RA, et al. Experimental treatment of Epstein-Barr virus-associated primary central nervous system lymphoma. *Cancer Res*. 2003;63(5):965-971.

45. Schorb E, Fox CP, Kasenda B, et al. Induction therapy with the MATRix regimen in patients with newly diagnosed primary diffuse large B-cell lymphoma of the central nervous system - an international study of feasibility and efficacy in routine clinical practice. *Br J Haematol*. 2020;189(5):879-887.

46. Munz C. Tumor microenvironment conditioning by abortive lytic replication of oncogenic gamma-herpesviruses. *Adv Exp Med Biol*. 2020;1225:127-135.

47. Gershburg E, Marschall M, Hong K, Pagano JS. Expression and localization of the Epstein-Barr virus-encoded protein kinase. *J Virol*. 2004;78(22):12140-12146.

48. Wille CK, Nawandar DM, Henning AN, et al. 5-hydroxymethylation of the EBV genome regulates the latent to lytic switch. *Proc Natl Acad Sci U S A*. 2015;112(52):E7257-E7265.

49. Radke J, Ishaque N, Koll R, et al. The genomic and transcriptional landscape of primary central nervous system lymphoma. *Nat Commun*. 2022;13(1):2558.

50. Kaulen LD, Denisova E, Hinz F, et al. Integrated genetic analyses of immunodeficiency-associated Epstein-Barr virus- (EBV) positive primary CNS lymphomas. *Acta Neuropathol*. 2023;146(3):499-514.

51. Skalska L, White RE, Franz M, Ruhmann M, Allday MJ. Epigenetic repression of p16(INK4A) by latent Epstein-Barr virus requires the interaction of EBNA3A and EBNA3C with CtBP. *PLoS Pathog*. 2010;6(6):e1000951.

52. Kraus RJ, Cordes BLA, Sathiamoorthi S, et al. Reactivation of Epstein-Barr virus by HIF-1α requires p53. *J Virol*. 2020;94(18):e00722-20.

53. Musukuma-Chifulo K, Siddiqi OK, Chilyabanyama ON, et al. Epstein-Barr virus detection in the central nervous system of HIV-infected patients. *Pathogens*. 2022;11(10):1080.